Electronic Supplementary Material (ESI) for RSC Advances.

Supplementary information
For
In-silico screening for oligopeptides useful as capture and reporting probes for interleukin-6 biosensing

Mohamed Mastouri,[a] Sabrine Baachaoui,[b] Amor Mosbah[b] and Noureddine Raouafi[a]*

[a] Sensors and Biosensors Group, Laboratory of Analytical Chemistry & Electrochemistry (LR99ES15), Faculty of Science, University of Tunis El Manar, 2092 Tunis El Manar, Tunisia.

[b] Laboratory BVBGR (LR11ES31), ISBST, University of Manouba, Biotechnopole Sidi Thabet, Ariana 2020, Tunisia.

*Corresponding author: email : Noureddine Raouafi (noureddine.raouafi@fst.utm.tn)

1. Selection of the peptides

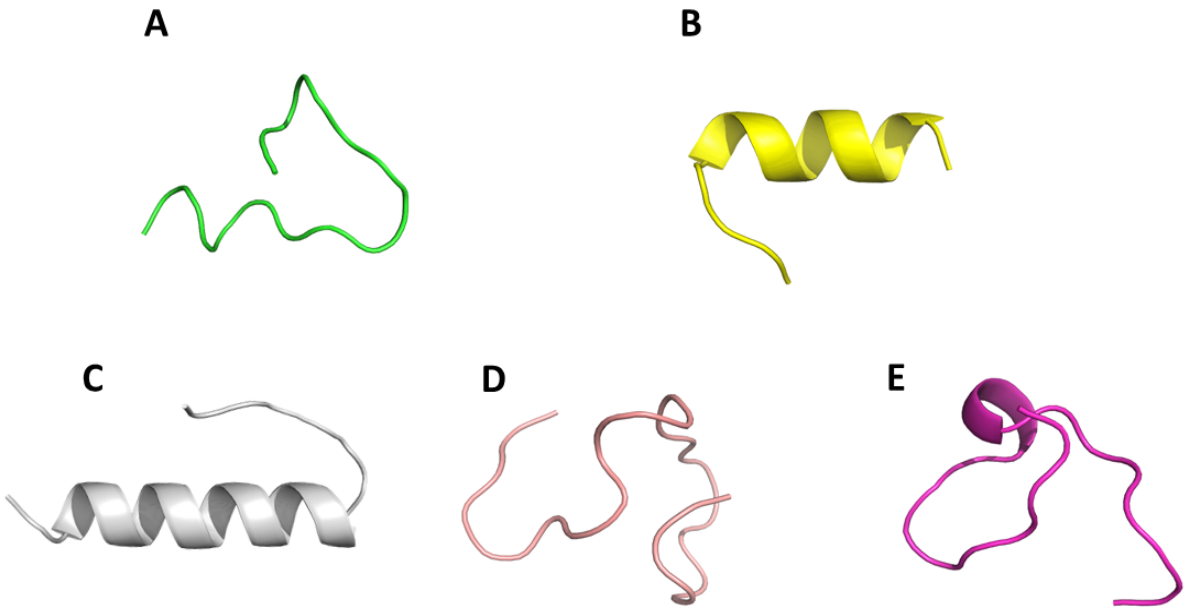

Figure S1. The snapshot of secondary structure of the different peptides: (A) CTE17, (B) CAY15, (C) CSE25, (D) CGF24 and (E) SGC20.

2. Simulation details

Table S1. Simulation details for the IL-6/peptide in solvent environment.

	System	Box Volume (nm^3)	Number of Biomolecule Atoms	Water Molecules	Simulation Time (ns)
IL6-peptide combination Simulation	CTE17	244.71	2925	6498	110
	CAY15	255.25	2971	6762	110
	CSE25	241.54	2936	6404	110
	CGF24	234.38	3032	6137	110
	SGC20	243.32	3107	6333	110

3. Docking

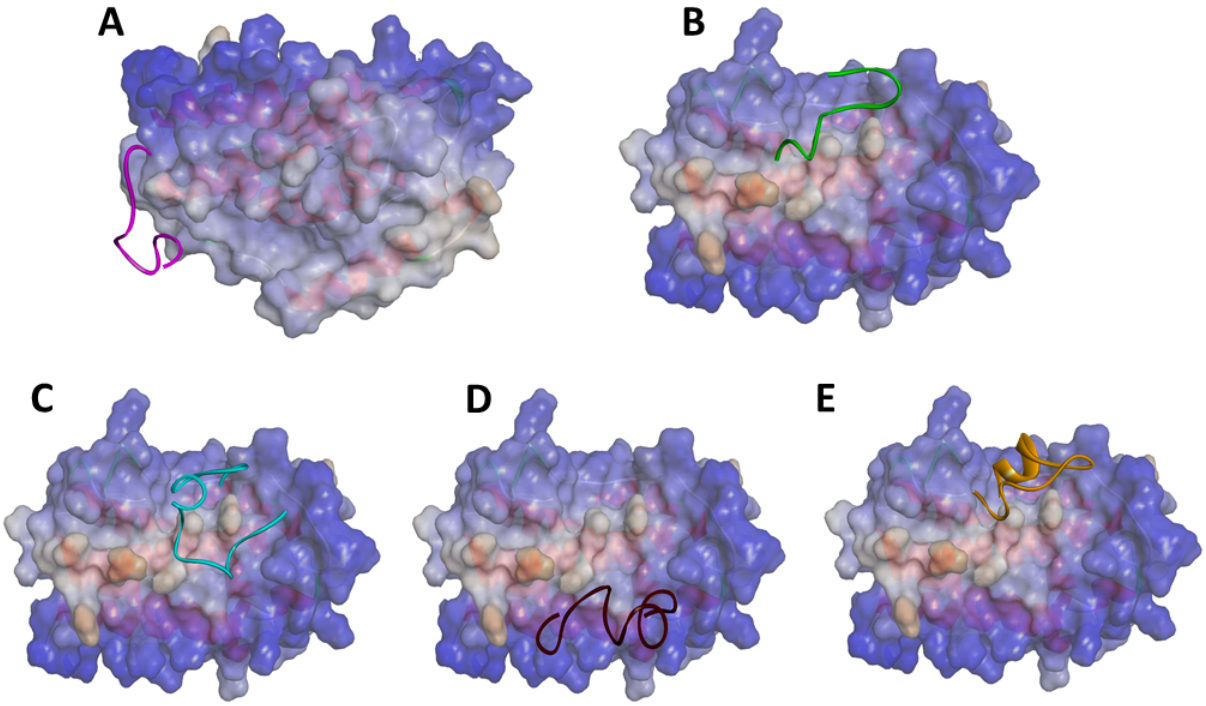

Figure S2. Final conformations and poses of the interactions between IL-6 and the peptides after docking : (A) CTE17, (B) CAY15, (C) CSE25, (D) CGF24 and (E) SGC20.

4. RMSD

CTE17/IL-6

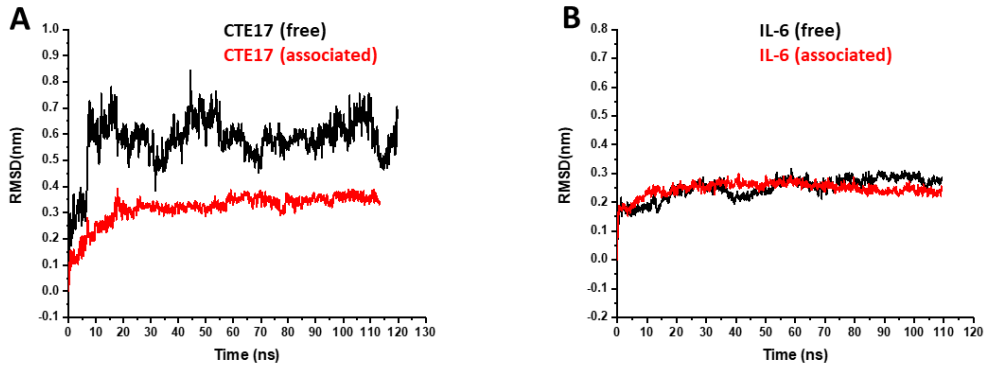

CAY15/IL-6

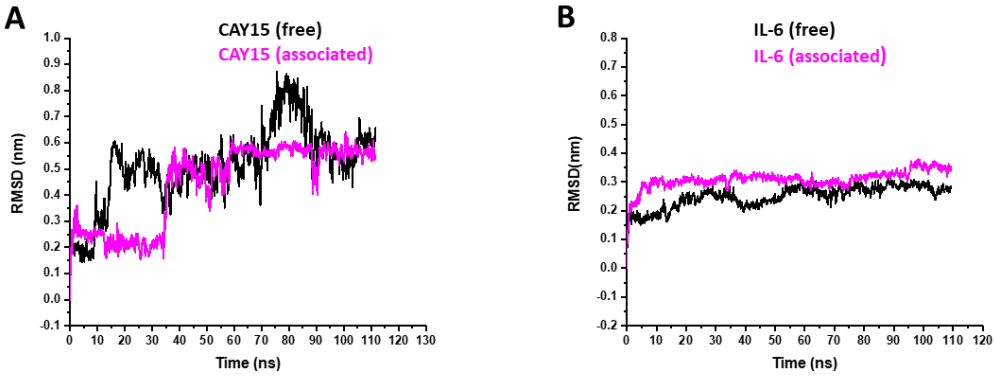

CSE25/IL-6

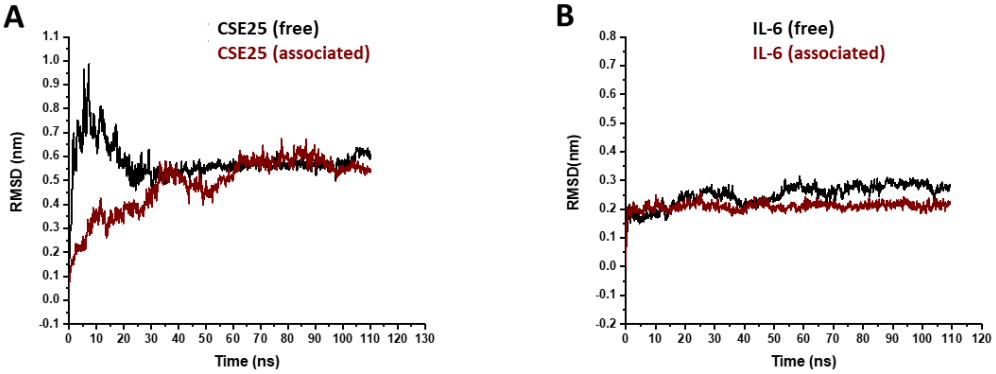

CGF24/IL-6

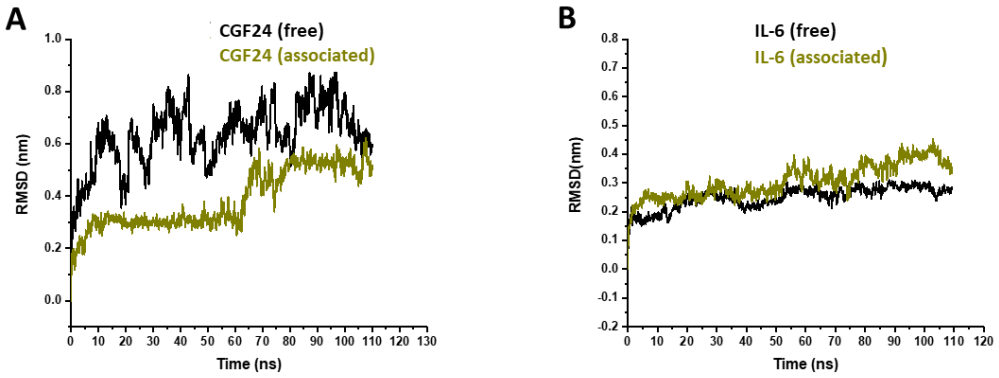

SGC20/IL-6

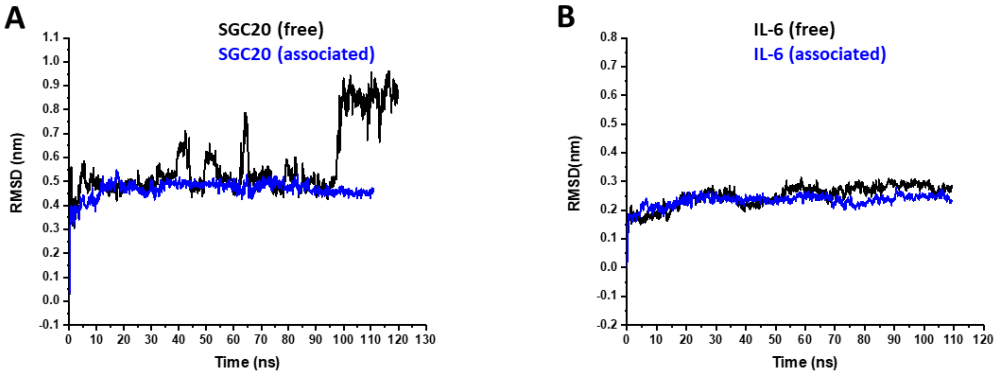

Figure S3. RMSD plots IL-6 and peptides during 110 ns MD simulation. (A) free peptide and associated peptide, (B) free IL-6 and associated IL-6.

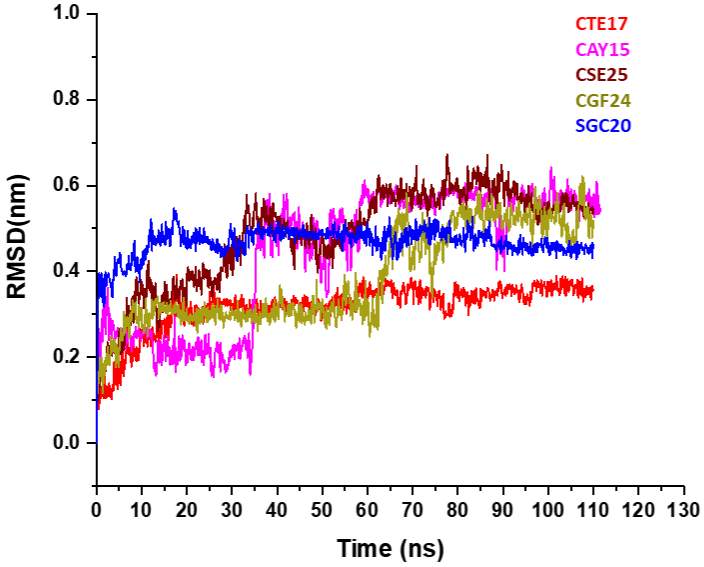

Figure S4. RMSD plots of associated peptides during the simulation tome.

5. Radius of Gyration

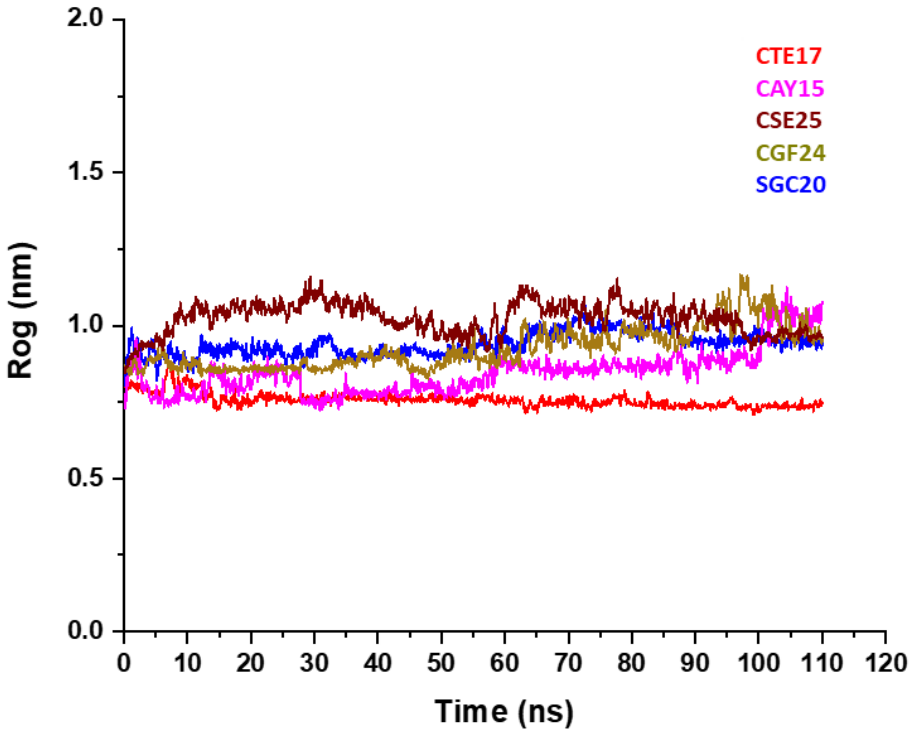

Figure S5. RoG plots of associated peptides during simulation time.

6. Hydrogen Bonds

Table S2. Interactions between the protein and the peptides during the 110 ns MD simulation. The relative frequency of the detected interactions H-bonds.

CTE17/IL-6

Donor	Acceptor	Occupancy
LYS110-Side	GLU17-Side	32.72%
LYS110-Side	SER4-Main	23.63%
ARG06-Side	ASP14-Side	31.75%
ASN114-Side	GLU17-Side	16.75%
ILE15-Main	LEU01-Main	14.46%

CAY15/IL-6

Donor	Acceptor	Occupancy
ARG161-Side	TYR15-Side	127.93%
LYS7-Side	SER151-Side	38.50%
TYR11-Side	SER158-Side	26.59%
LYS7-Side	GLU154-Side	56.85%
ASN8-Side	LEU46-Main	32.59%
ASN8-Side	GLU154-Side	30.80%
MET47-Main	ASN8-Side	32.14%
SER184-Side	TYR15-Side	25.07%
TYR9-Side	GLU51-Side	62.22%
ARG5-Side	GLU37-Side	93.82%

CSE25/IL-6

Donor	Acceptor	Occupancy
SER158-Side	GLU19-Side	10.57%
ARG150-Side	GLU25-Side	100.89%
ARG22-Side	ASP6-Side	89.79%
CYS1-Main	GLU37-Side	19.98%
ARG162-Side	ASP8-Side	59.06%
ARG150-Side	ASP21-Side	12.79%
SER19-Side	ASP6-Side	40.94%
ARG22-Side	ASP6-Main	18.12%
GLU33-Main	SER2-Main	12.79%
ARG164-Side	ASP8-Side	54.35%
LYS153-Side	ASP6-Side	20.60%
ARG161-Side	ASP21-Side	14.39%
LYS153-Side	GLU24-Side	12.26%
ARG161-Side	GLU19-Side	11.99%

CGF24/IL-6

Donor	Acceptor	Occupancy
ARG12-Side	PHE24-Side	14.59%
ALA3-Main	GLU33-Side	12.01%
ASN4-Main	GLU33-Side	25.53%
SER19-Side	ASP6-Side	17.88%
ASN5-Main	GLU33-Side	26.87%
ARG22-Side	ASP6-Side	102.58%
LYS153-Side	SER15-Main	12.01%
ARG17-Side	GLU37-Side	29.63%
SER15-Side	GLN157-Side	10.68%
ARG161-Side	PHE24-Side	20.82%
ARG17-Side	GLU41-Side	55.69%
CYS1-Main	GLU33-Side	12.90%

SGC20/IL-6

Donor	Acceptor	Occupancy
GLU51-Main	SER6-Side	39.51%
ARG12-Side	CYS20-Side	52.93%
ARG9-Side	GLU51-Side	12.06%
ARG161-Side	GLY16-Main	16.74%
SER19-Side	CYS20-Side	10.62%
ARG22-Side	CYS20-Side	31.32%
ARG12-Side	ASP19-Main	12.96%
LYS153-Side	CYS20-Side	13.50%
ARG61	ALA13-Main	10.53%

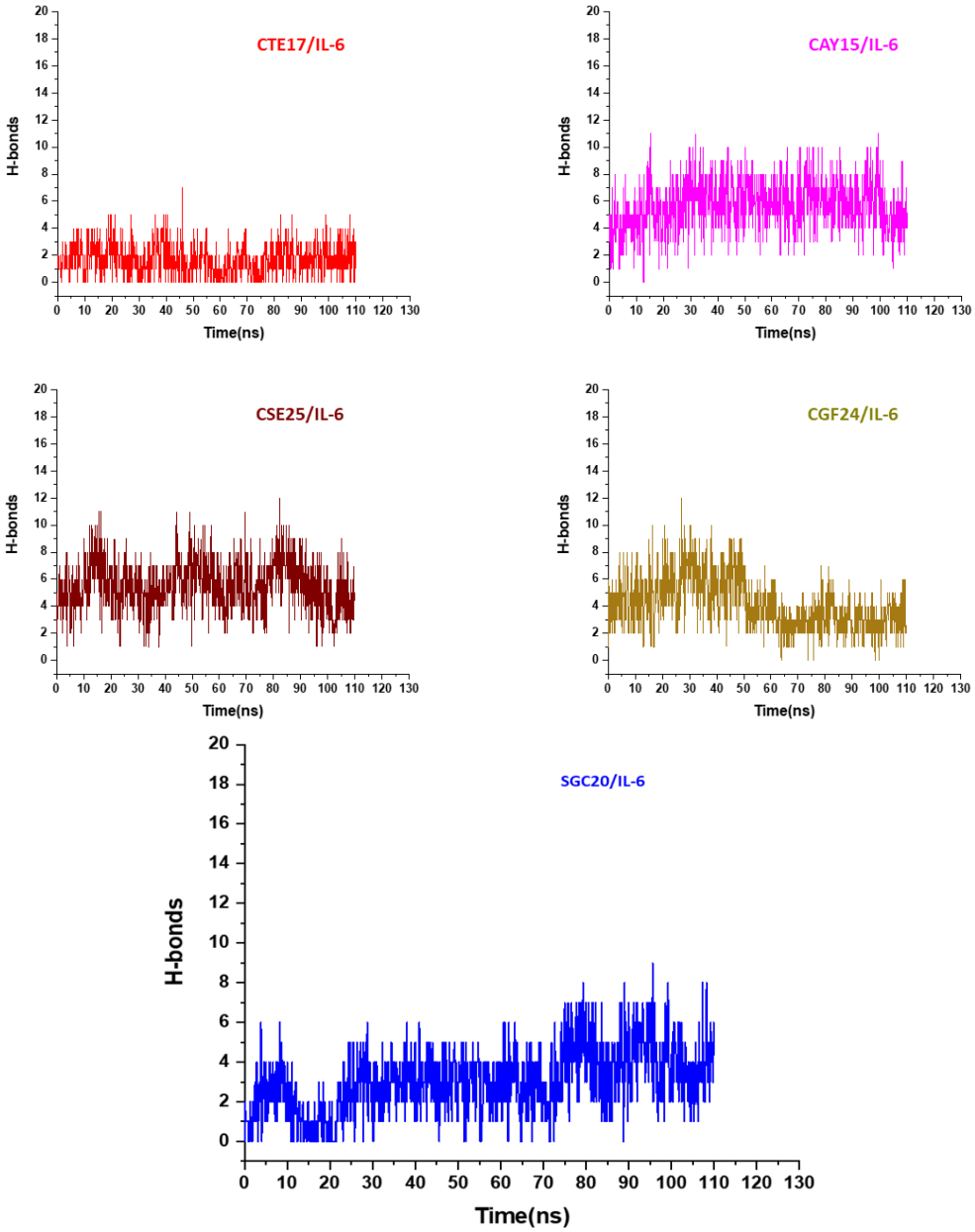

Figure S6. Number of hydrogen bonding interactions between IL-6 and the different peptides during 110 ns MD simulation for : CTE17/IL-6, CAY15/IL-6, CSE25/IL-6, CGF24/IL-6, SGC20/IL-6.

7. Hydrophobic interactions and salt bridges

Table S3. Interactions between the protein and the peptides during the last 40 ns MD simulation. The relative score of the detected hydrophobic and salt bridge interactions.

CTE17/IL-6

Contact	Type	Score
ARG25-NH2-IL-6_ASP14-CG-CTE17	Salt bridge	67%
ARG25-NH2-IL-6_ASP14-OD1-CTE17	Salt bridge	67%
ARG25-NH2-IL-6_ASP14-OD2-CTE17	Salt bridge	67%
LYS129-NZ-IL-6_GLU17-OT1-CTE17	Salt bridge	57%
LYS129-NZ-IL-6_GLU17-OT2-CTE17	Salt bridge	51%
PHE126-CZ-IL-6_ILE12-CG2-CTE17	hydrophobic	66%
PHE126-CE2-IL-6_ILE12-CG2-CTE17	hydrophobic	63%

CAY15/IL-6

Contact	Type	Score
GLU56-CD-IL-6_ARG5-NH2-CAY15	Salt bridge	77%
GLU56-CD-IL-6_ARG5-NE-CAY15	Salt bridge	50%
GLU56-OE1-IL-6_ARG5-NH2-CAY15	Salt bridge	76%
GLU56-OE1-IL-6_ARG5-NE-CAY15	Salt bridge	52%
GLU56-OE1-IL-6_ARG5-CZ-CAY15	Salt bridge	66%
GLU56-OE2-IL-6_ARG5-NH2-CAY15	Salt bridge	76%
GLU56-OE2-IL-6_ARG5-NE-CAY15	Salt bridge	55%
GLU56-OE2-IL-6_ARG5-CZ-CAY15	Salt bridge	67%
GLU173-CD-IL-6_LYS7-NZ-CAY15	Salt bridge	76%
GLU173-OE1-IL-6_LYS7-NZ-CAY15	Salt bridge	70%
GLU173-OE2-IL-6_LYS7-NZ-CAY15	Salt bridge	75%
GLU173-OE2-IL-6_LYS7-CE-CAY15	Salt bridge	52%
MET68-CB-IL-6_TYR9-CE2-CAY15	hydrophobic	67%
PHE75-CG-IL-6_TYR15-OH-CAY15	hydrophobic	50%
PHE75-CZ-IL-6_TYR15-OH-CAY15	hydrophobic	55%
PHE75-CD2-IL-6_TYR15-OH-CAY15	hydrophobic	64%
PHE75-CE2-IL-6_TYR15-OH-CAY15	hydrophobic	63%

CSE25/IL-6

Contact	Type	Score
ARG41-CZ-IL-6_ASP6-OD1-CSE25	Salt bridge	74%
ARG41-CZ-IL-6_ASP6-OD2-CSE25	Salt bridge	80%
ARG41-NH1-IL-6_ASP6-CG-CSE25	Salt bridge	72%
ARG41-NH1-IL-6_ASP6-OD1-CSE25	Salt bridge	85%
ARG41-NH1-IL-6_ASP6-OD2-CSE25	Salt bridge	78%
ARG41-NH2-IL-6_ASP6-CG-CSE25	Salt bridge	87%
ARG41-NH2-IL-6_ASP6-OD1-CSE25	Salt bridge	84%
ARG41-NH2-IL-6_ASP6-OD2-CSE25	Salt bridge	94%

ARG169-CZ-IL-6_GLU25-OT1-CSE25	Salt bridge	72%
ARG169-CZ-IL-6_GLU25-OT2-CSE25	Salt bridge	73%
ARG169-NH1-IL-6_GLU24-CB-CSE25	Salt bridge	50%
ARG169-NH1-IL-6_GLU25-OT1-CSE25	Salt bridge	84%
ARG169-NH1-IL-6_GLU25-OT2-CSE25	Salt bridge	82%
ARG169-NH2-IL-6_GLU25-OT2-CSE25	Salt bridge	84%
LYS172-CE-IL-6_GLU24-OE1-CSE25	Salt bridge	51%
LYS172-CE-IL-6_ASP6-OD1-CSE25	Salt bridge	61%
LYS172-NZ-IL-6_ASP6-OD1-CSE25	Salt bridge	68%
LYS172-NZ-IL-6_GLU24-OE1-CSE25	Salt bridge	53%
ARG183-CZ-IL-6_ASP8-CG-CSE25	Salt bridge	54%
ARG183-CZ-IL-6_ASP8-OD1-CSE25	Salt bridge	85%
ARG183-CZ-IL-6_ASP8-OD2-CSE25	Salt bridge	85%
ARG183-NH1-IL-6_ASP8-CG-CSE25	Salt bridge	87%
ARG183-NH1-IL-6_ASP8-OD1-CSE25	Salt bridge	92%
ARG183-NH1-IL-6_ASP8-OD2-CSE25	Salt bridge	92%
ARG183-NH2-IL-6_ASP8-CG-CSE25	Salt bridge	93%
ARG183-NH2-IL-6_ASP8-OD1-CSE25	Salt bridge	95%
ARG183-NH2-IL-6_ASP8-OD2-CSE25	Salt bridge	96%
ARG169-NH2-IL-6_GLU25-OT1-CSE25	Salt bridge	80%

CGF24/IL-6

Contact	Type	Score
ARG41-NE-IL-6_ASP6-CG-CGF24	Salt bridge	85%
ARG41-NE-IL-6_ASP6-OD1-CGF24	Salt bridge	93%
ARG41-NE-IL-6_ASP6-OD2-CGF24	Salt bridge	84%
ARG41-CZ-IL-6_ASP6-CG-CGF24	Salt bridge	56%
ARG41-CZ-IL-6_ASP6-OD1-CGF24	Salt bridge	89%
ARG41-CZ-IL-6_ASP6-OD2-CGF24	Salt bridge	83%
ARG41-NH2-IL-6_ASP6-CG-CGF24	Salt bridge	94%
ARG41-NH2-IL-6_ASP6-OD1-CGF24	Salt bridge	96%
ARG41-NH2-IL-6_ASP6-OD2-CGF24	Salt bridge	96%

SGC20/IL-6

Contact	Type	Score
ARG31-NH2-IL-6_ASP19-CB-SGC20	Salt bridge	53%
MET68-CG-IL-6_PHE3-CE1-SGC20	hydrophobic	63%
PHE75-CB-IL-6_PHE3-CE2-SGC20	hydrophobic	58%
PHE75-CD2-IL-6_PHE3-CD2-SGC20	hydrophobic	57%

8. CTE17/IL-6/CSE25 Sandwich System

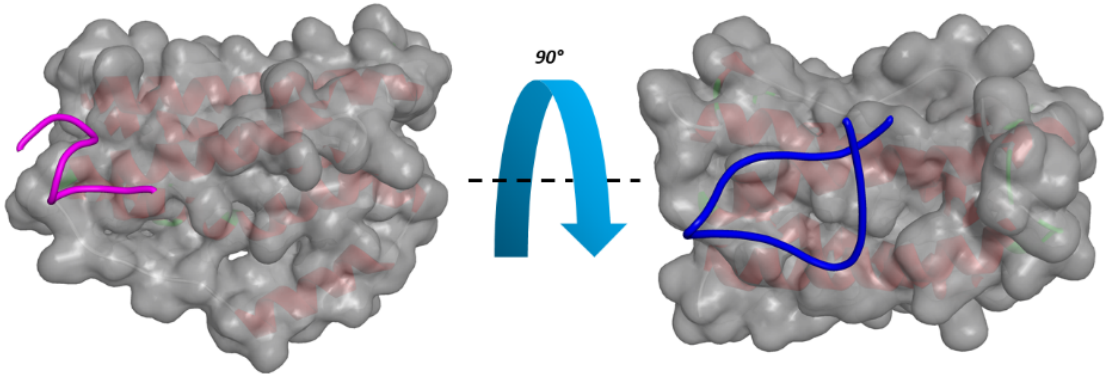

Figure S7. Final conformations and positions for CTE17 (magenta) and CSE25 (blue) extracted from the last frame of CTE17/IL–6 and CSE25/IL–6 MD simulations.

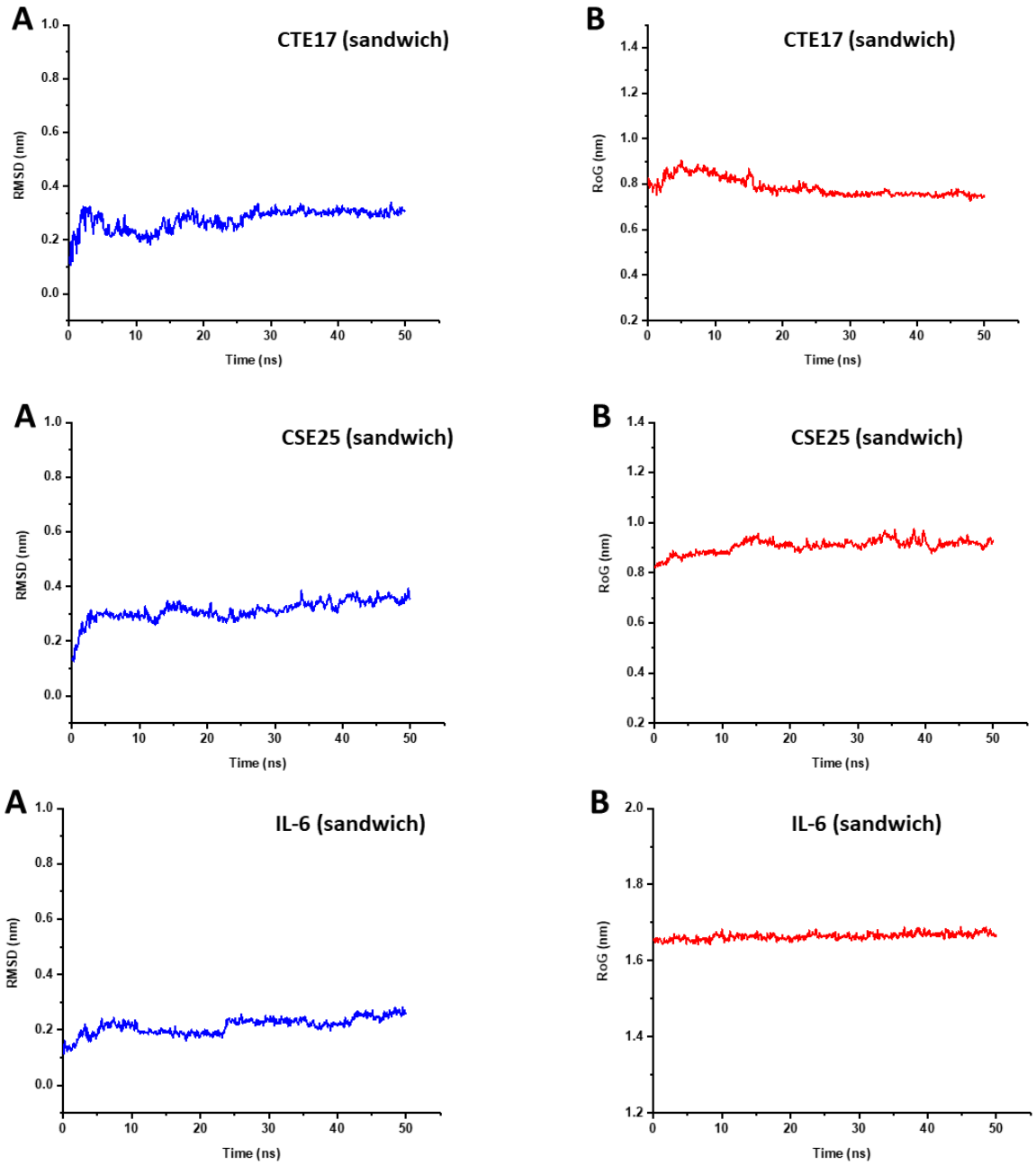

Figure S8. A) RMSD and B) RoG of the protein and peptides in sandwich system during 50 ns MD simulation.

9. Selectivity

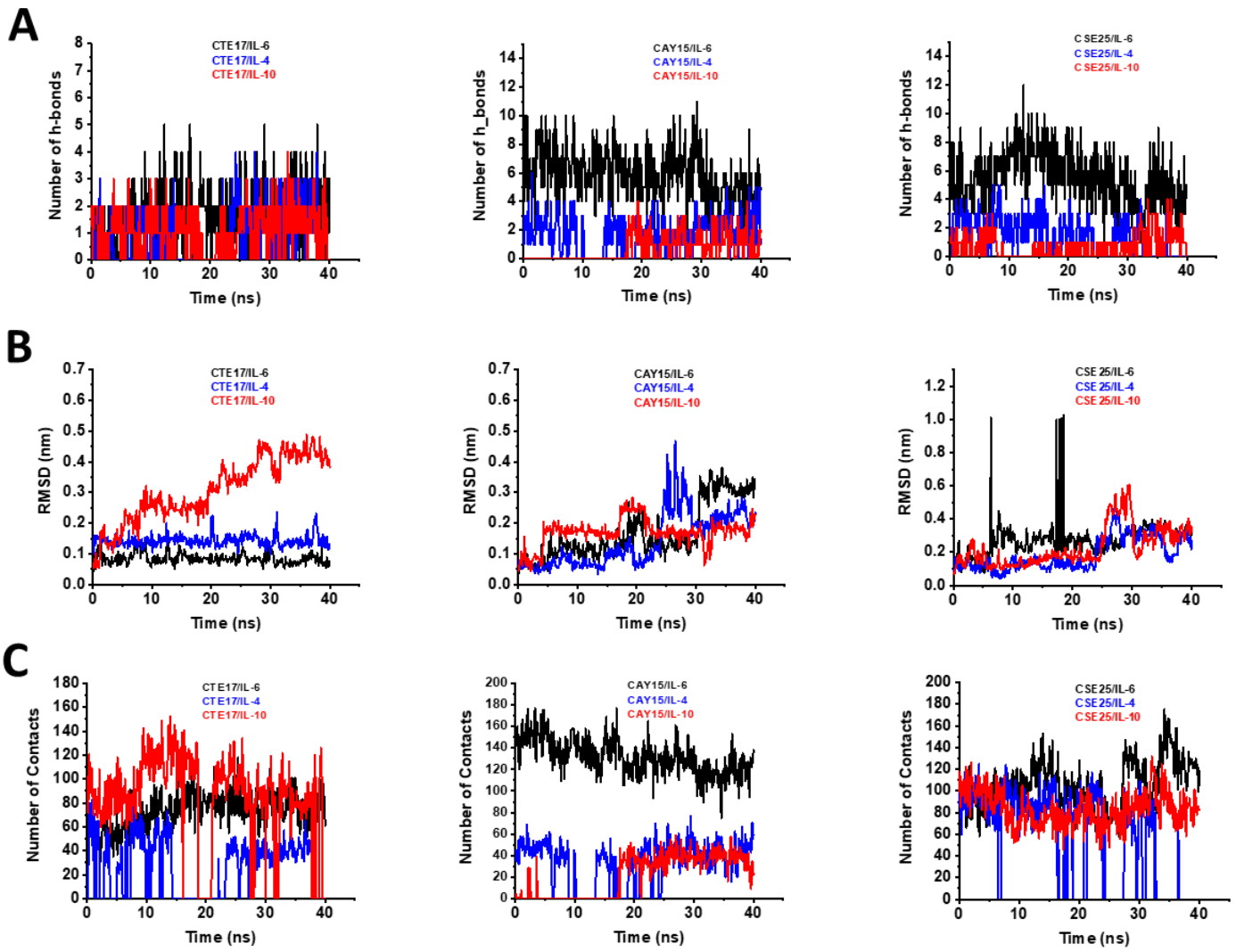

Figure S9. A) Number of h-bonds, B) RMSD and C) Number of contacts between the proteins and peptides during the last 40 ns of the MD simulation time.

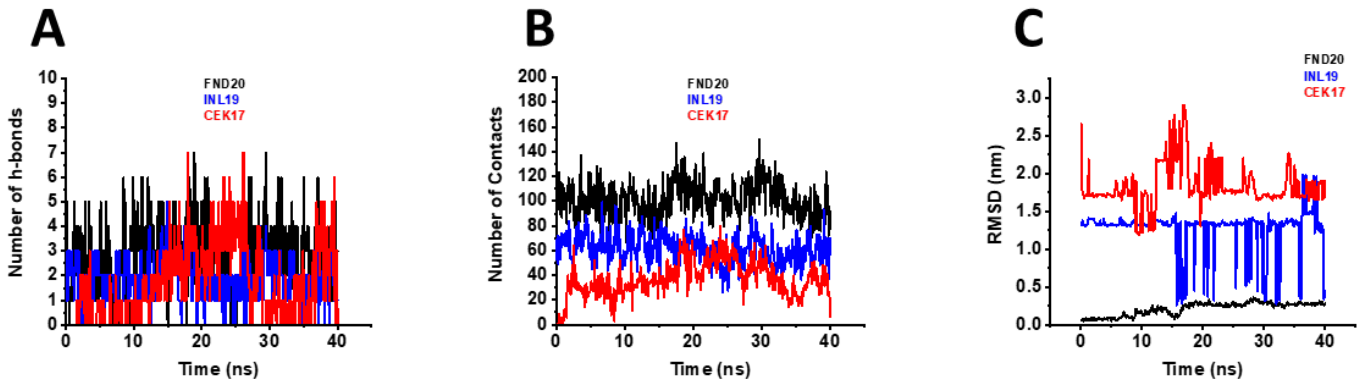

Figure S10. A) Number of h-bonds, B) RMSD and C) Number of contacts between the IL-6 and peptides during the last 40 ns of the MD simulation time.

Table S4. Comparison between the peptides associated with IL-6 during the last 40 ns of the MD simulation time.

Peptides	RMSD (nm)	Number of h-bonds	Number of contacts	Energy (kcal.mol^{-1})
FND20	2.13	2.8	101	-96.56
INL19	12.61	1.8	61	-12.52
CEK17	18.34	1.8	36	-4.03